On the Modelling of Fatigue Assessment and Lifetime Estimation in Marine Energies

Eguzkiñe Martinez-Puente [1], Ander Zarketa-Astigarraga [1], Jon Ander Esnaola[2], Alaitz Zabala[3], Manex Martinez-Astigarraga [1], Iñigo Llavori[3] and Markel Penalba[1,4]

***Abstract*—Due to the lack of a single operational point in offshore renewable energy (ORE) systems, fatigue assessment needs to cover the whole operational region, becoming more complex and time-consuming. Hence, the design of more efficient models is crucial. This study aims to evaluate the performance of various frequency-domain (FD) fatigue assessment methods for estimating the damage generated by stress loads characteristic to offshore environments. The examined spectral methods include Narrow-band approximation, Jiao-Moan, Dual narrow-band, Lotsberg, and Dirlik. The suitability of these methods is evaluated against the widely recognised time-domain Rainflow counting technique, which is assumed to be reliable, but computationally expensive. To expedite the comparative study, bimodal synthetic tension signals that represent mooring or dynamic cable loads occurring over the whole operational region of a ORE device are used. The results indicate that the Dirlik method exhibits a notable advantage in accurately reproducing rainflow damage estimates in bimodal processes, closely followed by the Dual narrow-band model.**

***Index Terms*—Offshore Renewable Energies, Mooring lines, Dynamic cables, Fatigue modelling, Frequency-domain, Bimodal processes.**

I. Introduction

ONE of the main challenges when designing offshore wave energy converters (WECs) is to achieve economic viability [1], [2]. This viability depends on two counter-productive aspects; enhancing energy absorption and generation, which requires increasing the WECs' motion as much as possible, while reducing the loads affecting critical elements, which requires a reduction in the motion [1]. Thus, it has become increasingly evident that a compromise between these two aspects must be reached.

This publication is part of the research project PID2021-124245OA-I00 funded by MCIN/AEI/10.13039/501100011033 and by ERDF A way of making Europe, and the research project funded by the Basque Government's ELKARTEK 2022 program under the grant No. KK-2022/00090. Finally, the authors from the Fluid Mechanics research group at Mondragon University are also supported by the Basque Government's Research Group Program under the grant No. IT1505-22.

[1] Fluid Mechanics Department, Mondragon University, Loramendi 4, 20500 Arrasate, Spain (email: eguzkine.martinez@alumni.mondragon.edu)

[2] Structural Mechanics and Design, Mondragon University, Loramendi 4, 20500 Arrasate, Spain

[3] Surface Technologies, Mondragon University, Loramendi 4, 20500 Arrasate, Spain

[4] Ikerbasque, Basque Foundation for Science, Euskadi Plaza 5, Bilbao, Spain

Digital Object Identifier:
https://doi.org/10.36688/ewtec-2023-490

For that purpose, it is crucial to have a reliable lifetime estimation methodology of critical components, enabling the optimisation of maintenance costs while also avoiding over-sizing of the parts that may lead to a more restrained performance of the WECs [3]. A complete structural integrity assessment is usually composed of an ultimate limit state (ULS) and a fatigue limit state (FLS) analysis. The former studies failure due to extreme loads and events, whereas the latter addresses the effect of cyclic loads, where failure may occur even below the material's yielding point [4]. Ultimate limit state assessment is performed only for the critical extreme conditions, whilst in fatigue, the whole operational region the device operates in must be taken into account. Consequently, more efficient models are required to study all the relevant loading conditions within the operating region.

Rainflow counting (RFC) [5] is a widely known time-domain (TD) technique and is assumed to be the most accurate estimate for fatigue as long as a sufficient amount of data, either experimental data from a real device or synthetic data from numerical simulations, is available, including relevant information for the behaviour of the system over the whole operational region. However, the RFC technique is also very time consuming to perform [6].

In contrast the frequency-domain (FD) analysis offers a faster alternative to RFC. This is because FD analysis involves deriving the statistical parameters of the TD response and using them in the various spectral methods available [7]. However, the damage estimates are dependent on the distributions adopted by each frequency domain approach [7], [8].

The primary objective of this study is to evaluate different FD methodologies to assess their suitability for estimating the damage experienced by WEC mooring lines. Specifically, the study aims to estimate the damage of mooring lines in WECs, comparing the results obtained with different methodologies under realistic wave climates. To accomplish this, the mooring response of the RM3 point absorber [9] is analysed and replicated using synthetic signals, which helps to expedite the analysis process. Subsequently, the damage obtained through the RFC method is used as the reference to compare the damage estimated via alternative FD approaches.

The reminder of the paper is organised as follows: Section II-A and Section II-B present the TD and FD approaches for fatigue assessment, respectively; Section III introduces the case study considered in this paper, briefly describing loading conditions and moor-

ing characteristics; Section IV shows the results of the analysed case study; and final remarks and conclusions are provided in Section V.

II. Fatigue evaluation scheme

A general fatigue damage assessment involves the following steps [10] (Fig. 1):

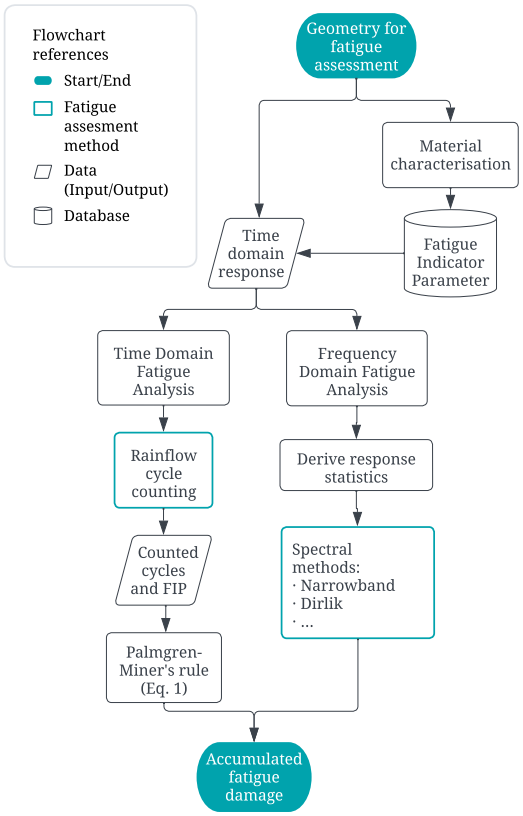

Fig. 1. Fatigue evaluation flowchart

- **1. Material Characterisation.** The first step consists on the characterisation of the material's fatigue behaviour to obtain the relationship between the stress or strain, and the fatigue life in cycles.
- **2. Fatigue Indicator Parameter.** The fatigue indicator parameter (FIP) is chosen based on the specific material and loading conditions, as a measure of the material's response to cyclic loading. Commonly used parameters include stress amplitude, strain amplitude, or a combination of both [10].
- **3. Loading History.** The next step is to obtain the loading history of the selected FIP. The loading history can be obtained from experimental data or numerical simulations.
- **4. Damage assessment.** Once the loading history is obtained, the fatigue analysis can be conducted either in the TD or the FD, depending on the available data and the analysis requirements.

A. Time-domain

When performing a time domain fatigue analysis, the loading history is divided into expected stress ranges associated with the number of cycles at that same value. Rainflow counting, developed by Matsuishi and Endo [5], is the most popular and used counting method to break down complex random loading data. This technique was inspired by the path followed by rain running down a pagoda roof, as illustrated in Fig. 2.

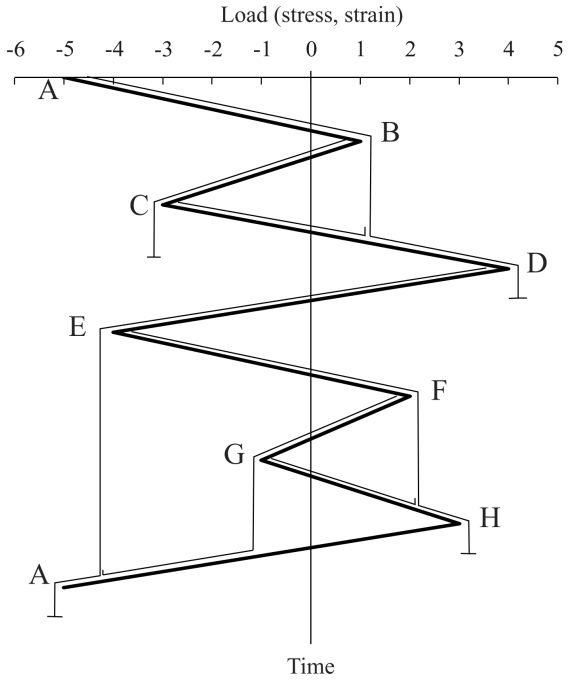

Fig. 2. Representation of the RFC of the loading history, [11].

The loading history is rotated 90º clockwise in Fig. 2, so that the sequence resembles a pagoda roof. According to RFC, the rain flow must start from a peak or valley and drip down until:

a) It falls opposite a larger maximum (or smaller minimum) point.

b) It meets a previous flow falling from above.

c) It falls below the roof.

Every time a rainflow reaches a termination point, a loading reversal (half cycle) is counted and assigned a stress range (the difference between its start and end positions). Lastly, half cycles of same range magnitude but opposite sense are paired up to count the number of complete cycles [11].

Once the cycles are identified, Miner's rule [12] is applied to estimate the accumulated damage caused by these cycles. The principle behind Miner's rule is that fatigue damage accumulates as a linear function of the number of cycles experienced by the material. Each cycle is assigned a damage value based on its amplitude and the endurance limit obtained from the corresponding stress-life (S-N) curve or strain-life (ε-N) curve of the material. The damage contribution of each cycle is then summed (see Eq. 1), indicating that the material is likely to fail due to fatigue if the cumulative damage exceeds a value of one.

$$D = \sum \frac{n_i}{N_i}, \tag{1}$$

where, n_i is the number of cycles within the magnitude range interval i and N_i is the number of cycles to failure at magnitude range i.

B. Frequency-domain

The diverse FD approaches offer a more computationally efficient alternative by analysing the loading spectrum that summarises all the relevant statistical properties of the loading history. Since RFC is recognised as the most accurate approach, these spectral methods aim to describe the statistical distribution of rainflow cycles [7].

Taking into consideration that the damage increment depends on constant amplitude fatigue properties by the S-N curve, Miner's equation can be expressed as:

$$D = \sum \frac{s_i^k}{C}, \tag{2}$$

where, s_i is the amplitude of the i-th counted cycle, k is the S-N curve slope and C is the fatigue strength.

In FD fatigue analyses it is common to refer to the damage in terms of the damage rate or the damage per unit time:

$$d = \frac{D}{T}, \tag{3}$$

where, T is the lifetime and D is the absolute amount of damage.

The damage intensity can then be derived from the integral of the cycle amplitude Probability Density Function (PDF) over the stress cycle amplitude [7], [8]:

$$d = \nu_{\mathrm{p}} C^{-1} \int_0^{+\infty} s^k p_{\mathrm{a}}(s) ds, \tag{4}$$

where, ν_{p} is the expected peak frequency, and $p_{\mathrm{a}}(s)$ is the cycle amplitude PDF.

The cycle amplitude probability estimate, usually implicitly determined using spectral moments methods, is based on the assumptions of Gaussianity of the process and its Power Spectral Density (PSD) [8].

Finding the true expression of the cycle distribution and connecting it to the random process's spectral density would be a more complete strategy. However, due to the intricate algorithm used for rainflow counting, the relationship between the cycle distribution and the process's TD (or FD) characteristics is extremely complicated to find. This is why, to this date, the true expression of the distribution is not known for broadband processes [7].

Some approaches address this problem either with theoretical considerations or by setting approximation methods, based on best fitting procedures on many simulation results [7].

In the most recent review of spectral methods, A. Zorman et al. [13] compared the accuracy of more than 20 spectral methods with several loading spectra from diverse applications. This research, however, focuses on evaluating only the performance for ORE applications.

On that note, only a few approaches have been chosen for examination:

i. The Narrow-band approximation method [14], further described in Section II-B1, was given special consideration due to its foundational nature, as many other methods are built upon this principle.
ii. Additionally, the Jiao-Moan method [15], further described in Section II-B2 was included in the analysis since offshore loads were considered in its development, making it particularly relevant for this study.
iii. Furthermore, the Dual narrow-band and Lotsberg methods, further described in Sections II-B3 and II-B4, respectively, were included due to their extensive utilisation in offshore specifications, such as those outlined by API and DNV [16]–[18].
iv. Lastly, the Dirlik method [19], further described in Section II-B5, was incorporated as a benchmark since it is widely accepted as a standard within the automotive industry, and it is known to give accurate results [20].

1) Narrow-band method: For strictly narrow-band Gaussian processes the cycle amplitude distribution coincides with the peak amplitude distribution, which, in this case, is a Rayleigh. The intensity of the counted cycles can also be taken as the mean zero up-crossing frequency, ν_0 [14] [7].

$$d_{\mathrm{NB}} = \nu_0 C^{-1} \left(\sqrt{2\lambda_0}\right)^k \Gamma\left(1 + \frac{k}{2}\right), \tag{5}$$

where λ_0 is the zero spectral moment and $\Gamma(\cdot)$ is the Euler gamma function.

2) Jiao-Moan method: Jiao and Moan developed a spectral method to calculate fatigue damage due to bimodal processes [15], including low and high frequency components, which are assumed to be related to current and wave effects, respectively. According to their findings, bimodal processes in the time domain exhibit clearly distinguishable small- and large-amplitude cycles. Hence, the total fatigue damage is the sum of the respective damages [13].

The small-amplitude damage is evaluated using the narrow-band approximation method (Eq. 5), considering solely the high-frequency response component.

The large-amplitude damage, however, is calculated by inserting the large-amplitude cycle distribution in Eq. 4. Large cycles are influenced by both, high and low frequency components. Therefore, the PDF is determined with the convolution of two Rayleigh distributions and the frequency is the mean zero up-crossing rate, $\nu_{0,\mathrm{P}}$:

$$\nu_{0,\mathrm{P}} = \lambda_1^* \nu_{0,1} \sqrt{1 + \frac{\lambda_2^*}{\lambda_1^*} \left(\frac{\nu_{0,2}}{\nu_{0,1}} \delta_2\right)^2}, \tag{6}$$

where subscripts 1 and 2 refer to the low and high frequency components respectively, $\lambda_i{}^*$ is the normalised variance of the component, and δ_2 is Vanmarcke's bandwidth parameter [21].

The closed-form solution is given in the form of a damage correction factor that is multiplied to the narrow-band damage of the whole process (calculated with Eq. 5):

$$\rho_{\text{JM}} = \frac{\nu_{0,\text{P}}}{\nu_{0,\text{Y}}}\left[{\lambda_1^*}^{\frac{k}{2}+2}\left(1-\sqrt{\frac{\lambda_2^*}{\lambda_1^*}}\right)+\sqrt{\pi\lambda_1^*\lambda_2^*}\frac{k\Gamma\left(\frac{k}{2}+\frac{1}{2}\right)}{\Gamma\left(\frac{k}{2}+1\right)}\right] + \frac{\nu_{0,2}}{\nu_{0,\text{Y}}}{\lambda_2^*}^{\frac{k}{2}}, \quad (7)$$

where $\nu_{0,\text{Y}}$ is the mean zero up-crossing rate of the whole process.

3) Dual narrow-band method: The dual narrow band approach is a highly recommended method by offshore standards such as DNV [17] and API [16]. It is based on the Jiao-Moan method, so the damage is calculated using equation 7. However, in these standards, instead of calculating Vanmarcke's bandwidth parameter, δ_2 is assumed equal to 0.1.

4) Lotsberg method: The Lotsberg method [18] is a spectral damage assessment technique designed specifically for bimodal stress processes. By employing the Narrow-band approximation method (II-B1), it effectively evaluates the low frequency and high frequency damages individually. Furthermore, it integrates these two separate damage calculations into a nonlinear combination to determine the total damage:

$$d_{\text{LB}} = d_{\text{NB,HF}}\left(1-\frac{\nu^+_{0,\text{LF}}}{\nu^+_{0,\text{HF}}}\right)+ \nu^+_{0,\text{LF}}\left[\left(\frac{d_{\text{NB,HF}}}{\nu^+_{0,\text{HF}}}\right)^{\frac{1}{k}}+\left(\frac{d_{\text{NB,LF}}}{\nu^+_{0,\text{LF}}}\right)^{\frac{1}{k}}\right], \quad (8)$$

where, $d_{\text{NB,HF}}$ and $d_{\text{NB,LF}}$ are obtained using Eq. 5 for the high frequency and low frequency components, respectively.

This method has recenlty become highly popular in DNV specifications [13] for offshore steel structures.

5) Dirlik method: Dirlik [19] developed an entirely empirical formula that approximates the rainflow amplitude distribution. This approach, based on extensive numerical simulations, is not supported by any kind of theoretical framework [7].

By analysing the density functions of the results obtained from his simulations, Dirlik concluded that the rainflow-range densities exhibit an exponential variation near the origin, while the mid-range features a Rayleigh function. Additionally, [19] also demonstrates the existence of a high-range standard Rayleigh distribution that explains why the rainflow-range densities did not trail off to zero as early. Hence, the proposed formulation is a sum of the three functions:

$$d_{\text{DK}} = \frac{\nu_{\text{P}}}{C}\lambda_0^{k/2}\left[G_1 Q^k \Gamma(1+k) + \left(\sqrt{2}\right)^k \Gamma\left(1+\frac{k}{2}\right)(G_2|R|^k+G_3)\right], \quad (9)$$

where G_1, G_2, G_3, R, Q and x_m are best fitting parameters:

$$x_m = \frac{\lambda_1}{\lambda_0}\left(\frac{\lambda_2}{\lambda_4}\right)^{1/2}, \qquad D_1 = \frac{2(x_m-\alpha_2^2)}{1+\alpha_2^2},$$
$$D_2 = \frac{1-\alpha_2-D_1+D_1^2}{1-R}, \qquad D_3 = 1-D_1-D_2, \quad (10)$$
$$Q = \frac{1.25(\alpha_2-D_3-D_2R)}{D_1}, \qquad R = \frac{\alpha_2-x_m-D_1^2}{1-\alpha_2-D_1+D_1^2}.$$

III. Case Study

This case study focuses on the analysis of the mooring system of the RM3 model [9]. In order to compare the different spectral models for damage assessment selected in Section II-B, the tension loading employed in this study is based on the specific characteristics and operational conditions of the RM3 device. By utilising the tension loading representative of the RM3, the performance and accuracy of the various methods in predicting fatigue damage for offshore applications can effectively be evaluated.

A. Mooring characteristics

The relevant geometrical data has been obtained from the information provided in the open-source WEC-Sim code [22]. The mooring system employed for the RM3 device consists of three mooring lines divided into two sections each with a submerged buoy in between (see Fig. 3). The relevant characteristics are summarised in Table I.

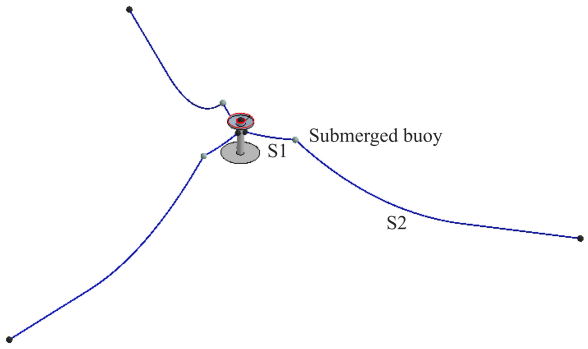

Fig. 3. RM3 mooring system representation.

TABLE I
Summary of the main parameters that define the mooring system setup for the RM3 model [22].

Diameter	[mm]	144
Linear density	[kg/m]	126
Line stiffness	[N]	583.38 10^6
S1 length	[m]	40
S2 length	[m]	240
Submerged buoy mass	[kg]	16755

As mentioned in Section II, to determine the fatigue damage of these stud chains, the S-N curve corresponding to R3 grade steel has been used. These properties have been obtained from the DNV specification for stud chains [17], as illustrated in Table II.

TABLE II
S-N CURVE PARAMETERS EMPLOYED IN THE CASE STUDY [17].

	C [MPa^k]	k
Stud chain	1.2 10^{11}	3

B. Loading conditions

Offshore structures are subjected to a complex and dynamic environment influenced by factors such as wind, waves, currents, etc. which contribute to the creation of different loading conditions.

Mooring tensions due to the hydrodynamic response of WECs are composed of two main frequency components: wave frequency (WF) and low frequency (LF). Fig. 4 depicts the two well-separated frequency components.

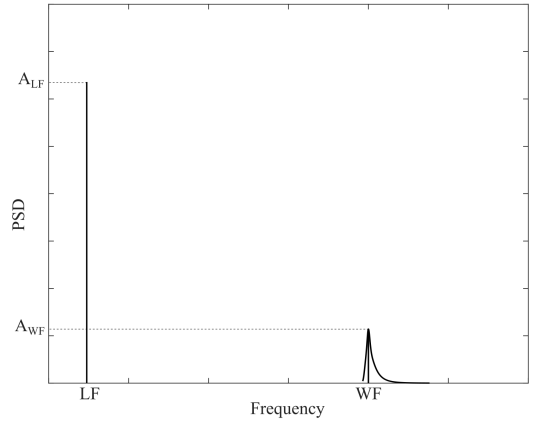

Fig. 4. Mooring line tension response power spectral density.

The wave frequency component represents the dynamic response of the mooring system to waves. It captures the oscillations and fluctuations in tension that occur as the waves pass by. These oscillations are typically of high frequency and short duration, corresponding to the characteristic periods of the waves.

On the other hand, the low frequency component represents the long-term variations in tension due to factors such as tidal forces, currents, and slow changes in environmental conditions. These variations occur over a much longer time scale compared to the wave frequency component.

As mentioned in Section I, to assess the fatigue damage on an offshore site, there is a wide range of sea states that must be considered. So as to speed the process up, synthetic tension signals inspired in hydrodynamic simulations have been generated instead of performing hydrodynamic simulations for each case.

1) Wave frequency tension signals: To generate the wave frequency components, first, the wave surface elevation is derived from the JONSWAP spectrum [23]. This spectrum is obtained based on the specified significant wave height (H_s), and peak period (T_p). For this study, 50 sea states have been produced with H_s ranging from 0.1 m to 14 m, and T_p from 4 s to 18 s, covering the whole operational region of a common WEC in most locations.

Once the wave surface elevation is acquired, it is multiplied by a factor of $5{\cdot}10^4$ to amplify its value and simulate the WF tension component. This amplification factor has been determined from observing mooring tension signals obtained from previous numerical simulations of the RM3 WEC via WEC-Sim, as described in Section III-A.

2) Low frequency tension signals: The low frequency signals are obtained from sine waves with a defined amplitude and frequency. These waves range in amplitude from $2{\cdot}10^4$ to 10^5 N with mean values between 10^5 and $8{\cdot}10^5$ N. Fig. 5 shows the realisation in time domain of one of the employed sea states.

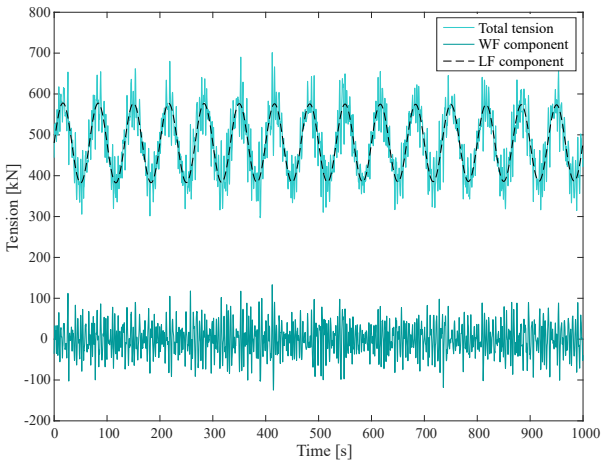

Fig. 5. Mooring line tension response split up into LF and WF components.

IV. RESULTS AND DISCUSSION

The damage results obtained from the spectral methods selected in Section II-B are compared to each other, with the reference (ground truth) being the damage estimated using the RFC method. Thus, the results presented include the relative damage difference as follows,

$$D_{\text{diff}} = \frac{D_{\text{FD}} - D_{\text{RFC}}}{D_{\text{RFC}}}, \tag{11}$$

which provides information on the accuracy of each FD method.

To ensure the reliability of the results, a convergence analysis has been conducted to determine the appropriate signal lengths for comparing the different methods. It is important to note that the results are influenced by the length of the analysed tension signals. Hence, this analysis assists in selecting the optimal signal lengths for a meaningful and accurate comparison among the various methods.

A. Effect of signal length

To accurately capture the statistical parameters of wave conditions, sea states are typically simulated over a three-hour duration in the time domain. However, to minimise signal lengths while maintaining reliable results, a convergence study has been conducted. This study examines the damage differences of the spectral

methods for various simulation lengths ranging from 100 seconds to almost three hours (10,000 seconds).

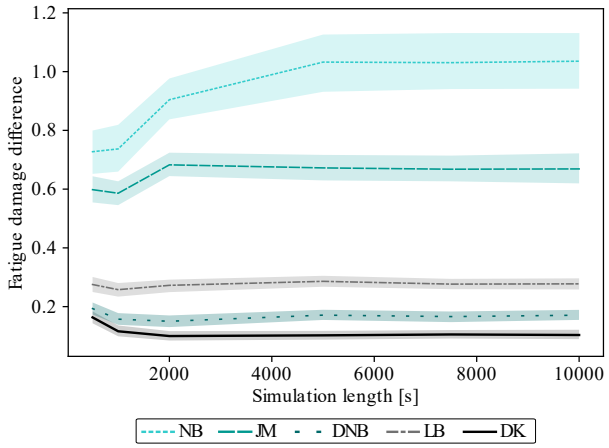

Fig. 6. Simulation length convergence patterns for each spectral method.

In Fig. 6, the convergence patterns of the damage differences are presented, along with a 95% confidence interval, for each spectral method. The Dirlik (DK), Jiao-Moan (JM), and Lotsberg (LB) methods converge at a simulation length of about 2000 seconds. On the other hand, the Narrow-band (NB), and Dual Narrow-band (DNB) methods require a slightly longer simulation length and converge at 5000 seconds. To ensure a fair and comparative analysis, all signals used in the study have been generated for a consistent length of 5000 seconds.

B. Comparison of fatigue models

In Fig. 7, the damage results for the simulated sea states are presented. The plot depicts the fatigue damage in the time domain on the horizontal axis and the fatigue damage of the frequency domain methods on the vertical axis. The RFC damage is represented as a reference line, indicating the target damage. Values below this line indicate non-conservative results, while values above indicate conservative results.

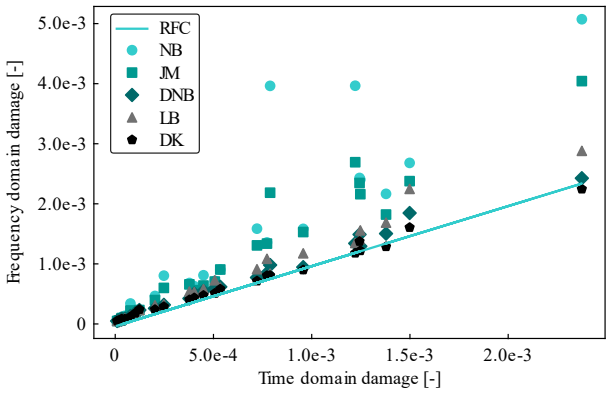

Fig. 7. Fatigue damage comparison of frequency and time domain methods.

With the exception of the Dirlik method, all other methods yield conservative (overestimated) results. However, the Dirlik method produces both over- and under-estimated damage values, although it appears to show the best agreement with the RFC method. Following closely behind are the Lotsberg and Dual Narrow-band methods, while the Jiao-Moan and Narrow-band methods exhibit greater dispersion.

To quantify the damage difference and determine which method yields the least relative difference, box-plot diagrams are utilised (see Fig. 8). Among the methods, the Narrow-band model exhibits the largest mean damage difference and the greatest dispersion of results. On the other hand, the Dirlik and Dual narrow-band methods yield the best results, with the Dirlik method demonstrating the smallest damage difference and dispersion. Table III shows the characteristic values of the box-plots, such as the mean, quartiles and interquartile range (IQR), for each spectral method.

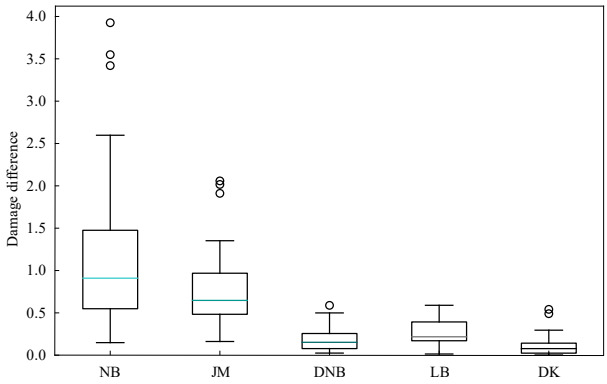

Fig. 8. Relative difference comparison for each spectral method.

TABLE III
DAMAGE MEAN RELATIVE DIFFERENCE AND BOX-PLOT QUARTILE VALUES IN PERCENTAGE.

	Mean	**Q1**	**Q3**	**IQR**
NB	91	55	148	93
JM	65	48	97	49
DNB	15	8	26	18
LB	22	17	40	23
DK	8	3	15	12

V. CONCLUSIONS

This paper presents an evaluation of various spectral methods for fatigue assessment, with the reference being the Rainflow counting (RFC) method in the time domain (TD). The study focuses on offshore loads, considering their unique characteristics and challenges.

Synthetic signals were successfully generated to efficiently represent realistic offshore loads, incorporating bimodal components comprising low frequency (LF) and wave frequency (WF) characteristics. These signals accurately represent the complex nature of offshore loading conditions.

Among the evaluated FD methods, the Dirlik method emerges as the most promising. It exhibits the smallest mean damage difference (8%) and result dispersion (12%), closely resembling the RFC damage. It is worth noting that, while generally conservative, it may occasionally yield non-conservative results.

On the other hand, the Dual narrow-band and Lotsberg methods, widely supported by offshore specifications, yield larger mean difference results (15% and 22%, respectively) as well as larger result dispersion (18% and 23%, respectively). However, these methods provide conservative results, ensuring a certain level of safety in fatigue assessment.

The results for the Narrow-band method clearly indicate that the assumption of offshore loads following a narrow-band distribution may be insufficient. This emphasises the importance of considering broader frequency ranges and more complex load characteristics in fatigue assessment for offshore structures.

Despite being specifically designed for bimodal loads characteristic in the offshore industry, the Jiao-Moan method does not yield satisfactory results in this study. Furthermore, when comparing the results obtained with the Dual narrow-band method, which is based on the Jiao-Moan method but utilises different Vanmarcke's bandwidth parameter values, it is evident that this parameter significantly influences the results. This underscores the importance of careful parameter selection and its impact on the accuracy of fatigue assessment.

In conclusion, this study provides valuable insight into the suitability of spectral methods for fatigue assessment in offshore applications. The Dirlik method shows promise for accurate fatigue assessment, while the Dual narrow-band and Lotsberg methods offer conservative results.

REFERENCES

[1] B. Guo and J. V. Ringwood, "A review of wave energy technology from a research and commercial perspective," *IET Renewable Power Generation*, vol. 15, no. 14, pp. 3065–3090, 2021, https://doi.org/10.1049/rpg2.12302.

[2] S. Astariz and G. Iglesias, "The economics of wave energy: A review," *Renewable and Sustainable Energy Reviews*, vol. 45, pp. 397–408, 2015, https://doi.org/10.1016/j.rser.2015.01.061.

[3] M. Penalba, J. I. Aizpurua, and A. Martinez-Perurena, "On the definition of a risk index based on long-term metocean data to assist in the design of marine renewable energy systems," *Ocean Engineering*, vol. 242, p. 110080, 2021. [Online]. Available: https://www.sciencedirect.com/science/article/pii/S0029801821014086

[4] J. E. Z. Shahroozi, M. Goteman, "Fatigue analysis of a point-absorber wave energy converter based on augmented data from a WEC-Sim model calibrated with experimental data," in *Trends in Renewable Energies Offshore*, C. G. Soares, Ed. Lisbon, Portugal: Taylor & Francis, 2022, https://doi.org/10.1201/9781003360773-102.

[5] M. Matsuishi and T. Endo, "Fatigue of metals subjected to varying stress," *Japan Society of Mechanical Engineers, Fukuoka, Japan*, vol. 68, no. 2, pp. 37–40, 1968.

[6] K.-T. Ma, Y. Luo, T. Kwan, and Y. Wu, "Chapter 6 - fatigue analysis," in *Mooring System Engineering for Offshore Structures*, K.-T. Ma, Y. Luo, T. Kwan, and Y. Wu, Eds. Gulf Professional Publishing, 2019, pp. 115–137, https://doi.org/10.1016/B978-0-12-818551-3.00006-5.

[7] D. Benasciutti, *Fatigue analysis of random loadings. A frequency-domain approach*. LAP Lambert Academic Publishing AG & Co KG, 2012.

[8] J. Slavič, M. Boltezar, M. Mrsnik, M. Cesnik, and J. Javh, *Vibration Fatigue by Spectral Methods: From Structural Dynamics to Fatigue Damage – Theory and Experiments*. Elsevier, 2020, https://doi.org/10.1016/C2019-0-04580-3.

[9] Reference model project (RMP) : Sandia energy. [Online]. Available: https://energy.sandia.gov/programs/renewable-energy/water-power/projects/reference-model-project-rmp/

[10] M. Muñiz-Calvente, A. Álvarez Vázquez, F. Pelayo, M. Aenlle, N. García-Fernández, and M. Lamela-Rey, "A comparative review of time- and frequency-domain methods for fatigue damage assessment," *International Journal of Fatigue*, vol. 163, p. 107069, 2022, https://doi.org/10.1016/j.ijfatigue.2022.107069.

[11] Y.-L. Lee and T. Tjhung, "Chapter 3 - rainflow cycle counting techniques," in *Metal Fatigue Analysis Handbook*, Y.-L. Lee, M. E. Barkey, and H.-T. Kang, Eds. Butterworth-Heinemann, 2012, pp. 89–114, https://doi.org/10.1016/B978-0-12-385204-5.00003-3.

[12] M. A. Miner, "Cumulative damage in fatigue," 1945, https://doi.org/10.1115/1.4009458.

[13] A. Zorman, J. Slavič, and M. Boltežar, "Vibration fatigue by spectral methods—a review with open-source support," *Mechanical Systems and Signal Processing*, vol. 190, p. 110149, 2023, https://doi.org/10.1016/j.ymssp.2023.110149.

[14] J. W. Miles, "On structural fatigue under random loading," *Journal of the Aeronautical Sciences*, vol. 21, no. 11, pp. 753–762, 1954, https://doi.org/10.2514/8.3199.

[15] G. Jiao and T. Moan, "Probabilistic analysis of fatigue due to gaussian load processes," *Probabilistic Engineering Mechanics*, vol. 5, no. 2, pp. 76–83, 1990, https://doi.org/10.1016/0266-8920(90)90010-H.

[16] R. API, "2sk," *Recommended practice for design and analysis of stationkeeping systems for floating structures.*, 2005.

[17] G. DNV, "Offshore standard-position mooring (dnvgl-os-e301)," *Edition July*, 2018.

[18] *Background for Revision of DNV-RP-C203 Fatigue Analysis of Offshore Steel Structure*, ser. International Conference on Offshore Mechanics and Arctic Engineering, vol. 24th International Conference on Offshore Mechanics and Arctic Engineering: Volume 3, 06 2005, https://doi.org/10.1115/OMAE2005-67549.

[19] T. Dirlik, "Application of computers in fatigue analysis." [Online]. Available: http://webcat.warwick.ac.uk/record=b1445503~S9

[20] J.-B. Park, J. Choung, and K.-S. Kim, "A new fatigue prediction model for marine structures subject to wide band stress process," *Ocean Engineering*, vol. 76, pp. 144–151, 2014, https://doi.org/10.1016/j.oceaneng.2013.11.002.

[21] E. H. Vanmarcke, "Properties of spectral moments with applications to random vibration," *Journal of the Engineering Mechanics Division*, vol. 98, no. 2, pp. 425–446, 1972, https://doi.org/10.1061/JMCEA3.0001593.

[22] WEC-sim (wave energy converter SIMulator) — WEC-sim documentation. [Online]. Available: http://wec-sim.github.io/WEC-Sim/master/index.html

[23] K. Hasselmann, T. P. Barnett, E. Bouws, H. Carlson, D. E. Cartwright, K. Enke, J. Ewing, A. Gienapp, D. Hasselmann, P. Kruseman *et al.*, "Measurements of wind-wave growth and swell decay during the joint north sea wave project (jonswap)." *Ergaenzungsheft zur Deutschen Hydrographischen Zeitschrift, Reihe A*, 1973.